

## Reverse Osmosis Separation of Amino Acids in Aqueous Solutions Using Porous Cellulose Acetate Membranes

TAKESHI MATSUURA and S. SOURIRAJAN, *Division of Chemistry, National Research Council of Canada, Ottawa, Canada, K1A 0R9*

### Synopsis

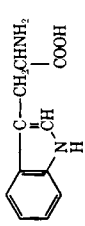
Polar and steric effects together govern the reverse osmosis separation of amino acids in single-solute aqueous solution systems. The solute transport parameter for the completely ionized aliphatic amino acids (with no additional polar groups other than one  $-\text{NH}_2$  and one  $-\text{COOH}$ ) in the  $pK_1$  range of 4.03 to 1.71 can be represented as a function of  $pK_1$  and the steric parameter  $\Sigma E_s$ . The latter parameter has a relatively greater influence with respect to the separation of zwitter ions. The effect of the polar parameter  $pK_1$  on solute separation increases with increase in the concentration of the ionic species  $\text{R}^+$  (or decrease in the concentration of the ionic species  $\text{R}^-$ ) in the feed solution. The effect of the presence of additional polar groups in the amino acid molecule is to increase its basicity. Experiments with *p*-aminobenzoic acid solutions indicate that the undissociated acid is preferentially sorbed at the membrane-solution interface. With respect to both aliphatic and aromatic amino acid ions, solute separation is in the order  $\text{R}^- > \text{R}^\pm > \text{R}^+$  for the cellulose acetate membrane material studied.

### INTRODUCTION

The physicochemical criteria for reverse osmosis separations of carboxylic acids and amines in single-solute aqueous solution systems using Loeb-Sourirajan-type porous cellulose acetate membranes have been discussed.<sup>1-3</sup> This paper is concerned with the development of criteria for such separations appropriate for amino acids. Amino acids are present in many biochemical systems, and they are essential constituents of protein molecules present in natural food substances. In aqueous solutions, amino acids exist (to different extents) as amphoteric dipolar ions (zwitter ions); the physicochemical criteria for the reverse osmosis separation of such ions may be expected to govern, in part, the applications of the process in food processing, biochemistry, and medicine.

Consequently, this work is of both theoretical and practical interest. Kamizawa et al.<sup>4</sup> studied the reverse osmosis separations of three aliphatic and two aromatic amino acids using porous cellulose acetate membranes of the general type used in this work. They came to the conclusion, already illustrated in reference 1, that solute separation increased with increase in the degree of dissociation of the acid. This work is a more extensive study

TABLE I  
 Data on Amino Acids Used

Solute		Solute									
Solute no.	Name	Formula	Molecular weight	$pK_1$	$pK_2$	$pK_2$	$E_s$	$V_1$ , cm <sup>3</sup> /g- mole	$D_{AB} \times 10^6$ , cm <sup>2</sup> /sec	$D_{AB} \times 10^6$ , cm <sup>2</sup> /sec	$k \times 10^4$ sec
Amino acid with equal number of basic and acidic group											
1	Glycine	CH <sub>2</sub> (NH <sub>2</sub> )COOH	75.07	2.31	9.72	7.73	-0.07	78.0	1.069	1.064	43.9
2	DL-Alanine	CH <sub>3</sub> CH(NH <sub>2</sub> )COOH	89.09	2.39	9.72	7.80	-0.47	100.2	0.919	0.910	39.2
3	DL-Valine	(CH <sub>3</sub> ) <sub>2</sub> CHCH(NH <sub>2</sub> )COOH	117.15	2.32	9.62		-2.19	144.6	0.738		33.8
4	DL-Leucine	(CH <sub>3</sub> ) <sub>2</sub> CHCH <sub>2</sub> CH(NH <sub>2</sub> )COOH	131.17	2.34	9.64	7.63	-1.15	166.8	0.677		32.0
5	DL-Isoleucine	C <sub>2</sub> H <sub>5</sub> CH(CH <sub>3</sub> )CH(NH <sub>2</sub> )COOH	131.17	2.26	9.62		-2.30	166.8	0.677		32.0
6	DL-Phenylalanine	C <sub>6</sub> H <sub>5</sub> CH <sub>2</sub> CH(NH <sub>2</sub> )COOH	165.19	1.83	9.13		-1.19	188.8	0.629		30.4
7	DL-Tyrosine	p-HOC <sub>6</sub> H <sub>4</sub> CH <sub>2</sub> CH(NH <sub>2</sub> )COOH	181.19	2.20	9.11			196.2	0.614		30.0
8	DL-Threonine	CH <sub>3</sub> CHOHCH(NH <sub>2</sub> )COOH	119.12	2.15	9.12			129.8	0.787		35.4
9	DL-Serine	CH <sub>2</sub> OHCH(NH <sub>2</sub> )COOH	105.09	2.21	9.15			107.6	0.881		38.1
10	L-Proline	H <sub>2</sub> C—CH <sub>2</sub>   NH	115.13	1.99	10.60		-0.51	127.2	0.797		35.7
11	DL-Tryptophane		204.23	2.38	9.39			222.6	0.570		28.5
12	DL-Methionine	CH <sub>3</sub> SCH <sub>2</sub> CH <sub>2</sub> CH(NH <sub>2</sub> )COOH	149.21	2.28	9.21			170.2	0.669		31.7
13	L-Cystine	SCH <sub>2</sub> CH(NH <sub>2</sub> )COOH   SCH <sub>2</sub> CH(NH <sub>2</sub> )COOH	240.29	<1	2.1			244.2	0.539		27.5

14	L-Cysteine	$\text{HSCH}_2\text{CH}(\text{NH}_2)\text{COOH}$	121.15	1.71	8.33				125.8	0.802	35.8
15	$\alpha$ -Aminoisobutyric acid	$(\text{CH}_2)_2\text{C}(\text{NH}_2)\text{COOH}$	103.12	2.39*	—			-1.54	122.4	0.816	36.2
16	DL-Norvaline	$\text{CH}_3(\text{CH}_2)_2\text{CH}(\text{NH}_2)\text{COOH}$	117.15	2.36	9.72			-1.21	144.6	0.738	33.9
17	DL-Norleucine	$\text{CH}_3(\text{CH}_2)_3\text{CH}(\text{NH}_2)\text{COOH}$	131.17	2.39	9.76			-1.22	166.8	0.677	32.0
18	DL- $\alpha$ -Aminocaproic acid	$\text{CH}_3(\text{CH}_2)_5\text{CH}(\text{NH}_2)\text{COOH}$	159.23	2.39*	—			-1.22	211.2	0.588	29.1
19	$\beta$ -Alanine	$\text{NH}_2\text{CH}_2\text{CH}_2\text{COOH}$	89.09	3.60	10.19	9.13		-0.36	100.2	0.919	39.2
20	$\gamma$ -Amino- <i>n</i> -butyric acid	$\text{NH}_2\text{CH}_2\text{CH}_2\text{CH}_2\text{COOH}$	103.12	4.03	10.56	9.71		-0.39	122.4	0.816	36.2
21	$\epsilon$ -Amino- <i>n</i> -caproic	$\text{NH}_2(\text{CH}_2)_5\text{COOH}$	131.17	4.43	10.75	10.37			166.8	0.677	32.0
22	Sarcosine	$\text{CH}_3\text{NHCH}_2\text{COOH}$	89.09	2.23	10.01			-0.36	101.7	0.911	39.0
23	Betaine	$(\text{CH}_3)_3\text{N}^+\text{CH}_2\text{COO}^-$	117.15	1.88	—			-1.74	149.7	0.723	33.4
24	<i>m</i> -Aminobenzoic acid	$m\text{-NH}_2\text{C}_6\text{H}_4\text{COOH}$	137.13	3.04	4.79	3.56			144.4	—	0.774
25	<i>p</i> -Aminobenzoic acid	$p\text{-NH}_2\text{C}_6\text{H}_4\text{COOH}$	137.13	2.32	4.92	2.38			144.4	0.855	0.843
26	Basic amino acid										
26	L-Lysine	$\text{H}_2\text{N}(\text{CH}_2)_4\text{CH}(\text{NH}_2)\text{COOH}$	146.19	2.20	8.90				181.0	0.645	31.0
27	L-Arginine	$\text{NH}_2$   $\text{NH}=\text{C}-\text{NH}(\text{CH}_2)_3\text{CH}(\text{NH}_2)\text{COOH}$									
		$\text{CH}=\text{C}-\text{CH}_2\text{CH}(\text{NH}_2)\text{COOH}$	174.21	2.18	9.09				205.0	0.598	29.5
28	L-Histidine	$\text{N}$ $\text{NH}$   $\diagdown$ $\text{CH}$	155.16	1.78	5.97				112.3	0.859	37.5
	Acid amino acid										
29	L-Aspartic acid	$\text{HOOCCH}_2\text{CH}(\text{NH}_2)\text{COOH}$	133.10	1.88	3.65				134.4	0.771	34.9
30	L-glutamic acid	$\text{HOOCCH}_2\text{CH}_2\text{CH}(\text{NH}_2)\text{COOH}$	147.13	2.19	4.25				156.6	0.704	32.8

\* Estimated from  $\text{p}K_1$ -vs.-Taft number correlation.<sup>1</sup>

of the subject, involving 30 amino acids. This work illustrates quantitative correlations of solute separation data with physicochemical parameters characterizing the chemical structure of simple aliphatic amino acids and establishes methods of predicting solute separation in reverse osmosis based on such correlations.

## EXPERIMENTAL

The amino acids used are listed in Table I along with some of their physicochemical data pertinent to this work. In reverse osmosis experiments, solute concentrations in the feed solutions were in the range 0.0005 to 0.003 g-mole/l. (73 to 243 ppm of solute), and the operating pressure was 250 or 500 psig. Laboratory-made Batch 316 (10/30)-type cellulose acetate membranes<sup>5,6</sup> were used. The apparatus and experimental procedure used were the same as described before.<sup>1</sup> The feed flow rate used was about 400 cc/min in all cases, which corresponded to a mass transfer coefficient of  $57 \times 10^{-4}$  cm/sec for 1500 ppm NaCl-H<sub>2</sub>O feed solution. All reverse osmosis data are for single-solute systems. The specifications of the film samples used are given in Table II in terms of the pure water permeability constant  $A$  (in g-mole H<sub>2</sub>O/cm<sup>2</sup> sec atm) and solute transport parameter  $(D_{AM}/K\delta)$  for NaCl at the given operating pressure.

All experiments were of the short-run type, and they were carried out at the laboratory temperature (23–25°C). The reported product rates are those corrected to 25°C using the relative viscosity and density data for pure water. In all experiments, the terms "product" and "product rate" refer to membrane permeated solutions.

The fraction solute separation  $f$  with respect to each amino acid was obtained from the relation

$$f = \frac{\text{solute ppm in feed} - \text{solute ppm in product}}{\text{solute ppm in feed}}$$

A Beckman total carbon analyzer, Model 915, was used to measure the concentrations of the amino acid in the feed and product solutions. In each

TABLE II  
Film Specifications and Some Performance Data

Film no.	Operating pressure	Specifications		Performance data <sup>a</sup>	
		$A \times 10^6$ , g-mole/ cm <sup>2</sup> sec atm	$(D_{AM}/K\delta) \times$ $10^4$ , cm/sec	Solute sepn., %	Product rate, <sup>b</sup> g/hr
2	250	3.79	5.14	93.4	28.9
5	250	8.32	63.94	70.6	64.8
6	250	11.11	111.9	58.3	85.9
7	500	5.98	43.30	82.6	95.2
8	500	5.09	25.18	86.8	80.8

<sup>a</sup> Feed: 1500 ppm NaCl-H<sub>2</sub>O.

<sup>b</sup> Area of film surface: 7.6 cm<sup>2</sup>;  $k = 57 \times 10^{-4}$  cm/sec.

experiment, the pure water permeation rate (*PWP*), and product rate (*PR*), in grams per hour per given area of film surface (7.6 cm<sup>2</sup> in all cases in this work), and solute separation *f* were determined at the specified operating conditions. The solute numbers given in all figures in this paper are the same as those given in Table I. In the solute concentration range used in this work, the osmotic pressure of the feed solution was negligible in all cases.

## RESULTS AND DISCUSSION

### Calculation of Diffusivity of Solutes in Water

Data on diffusivity of solutes in water ( $D_{AB}$ ) are needed for the calculation of mass transfer coefficients (*k*) on the high-pressure side of the membrane during reverse osmosis experiments. In the absence of actual experimental data, the values of  $D_{AB}$  can be calculated, as before,<sup>8</sup> from the empirical equation of Wilke and Chang<sup>9</sup>:

$$D_{AB} = 7.4 \times 10^{-8} \frac{(\chi M)^{1/2} T}{\mu V_1^{0.6}} \quad (1)$$

where  $\chi$  = "association" parameter of solvent (=2.6 for water);  $M$  = molecular weight of solvent (=18.02 for water); and  $T$  = temperature, °K (=298°K);  $\mu$  = viscosity of solution, centipoises (=0.8937 centipoise for pure water); and  $V_1$  = molal volume of solute at normal boiling point, cm<sup>3</sup>/g-mole, obtained by summation of atomic volume data listed in the literature.<sup>10</sup>

There is, however, some question whether the values of  $D_{AB}$  so calculated are valid for completely dissociated amino acids, because the literature values<sup>11</sup> of  $D_{AB} \times 10^5$  (in cm<sup>2</sup>/sec) for glycine, DL-alanine, and  $\beta$ -alanine are 1.064, 0.910, and 0.933, respectively, compared to the values of 1.238, 1.065, and 1.065 calculated from eq. (1). On the other hand, the literature value<sup>11</sup> of  $D_{AB} \times 10^5$  for *p*-aminobenzoic acid, which is composed largely of the uncharged form in aqueous solution, is 0.843 compared to the value of 0.855 calculated from eq. (1). Consequently, it seems reasonable to use eq. (1) for calculating the  $D_{AB}$  values of undissociated amino acids and to use an appropriate multiplying factor to obtain the applicable values of  $D_{AB}$  from those calculated from eq. (1), with respect to completely dissociated amino acids. Since the ratios of the calculated to actual values of  $D_{AB}$  for glycine, DL-alanine, and  $\beta$ -alanine are 0.859, 0.854, and 0.876, respectively, an average of these ratios (=0.863) seems to be a reasonable multiplying factor for this purpose. Therefore, for obtaining the applicable  $D_{AB}$  values for completely dissociated amino acids in aqueous solutions, the Wilke-Chang equation was modified as follows:

$$D_{AB} = 0.863 \times 7.4 \times 10^{-8} \frac{(\chi M)^{1/2} T}{\mu V_1^{0.6}} \quad (2)$$

The values of  $D_{AB}$  used in this work, as obtained from eq. (1) or (2), are listed in Table I.

### Calculation of Solute Transport Parameter ( $D_{AM}/K\delta$ ) for Amino Acids

The values of  $D_{AM}/K\delta$  for each solute were calculated from the experimental solute separation ( $f$ ) and product rate  $PR$  data. The procedure used for this calculation was the same as that used before for alcohols.<sup>8</sup> For each experiment, the mass transfer coefficient  $k$  on the high-pressure side of the membrane was calculated from the relation

$$k = k_{\text{ref}} \left[ \frac{D_{AB}}{(D_{AB})_{\text{ref}}} \right]^{2/3} \quad (3)$$

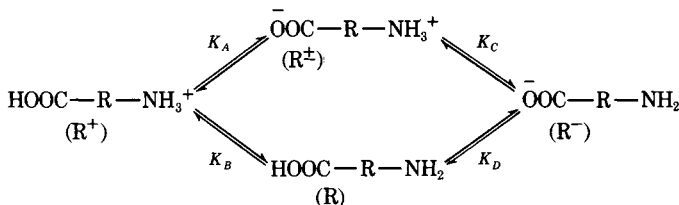
where  $k_{\text{ref}}$  = mass transfer coefficient on the high-pressure side of the membrane for the reference solution system 1500 ppm NaCl-H<sub>2</sub>O ( $= 57 \times 10^{-4}$  cm/sec), and  $(D_{AB})_{\text{ref}}$  and  $D_{AB}$  refer to diffusivity of sodium chloride and amino acid, respectively, in water. The values of  $k$  so obtained for the solution systems used in this work are given in Table I. Using the applicable value of  $k$  and the experimental  $f$  and  $PR$  data, the value of  $D_{AM}/K\delta$  for each solute was calculated from the relation:

$$D_{AM}/K\delta = \frac{PR}{3600 Sd} \frac{(1-f)}{f} \left[ \exp \left\{ \frac{PR}{3600 Skd} \right\} \right]^{-1} \quad (4)$$

where  $S$  = effective membrane area (cm<sup>2</sup>) and  $d$  = solution density (g/cm<sup>3</sup>).

### Calculation of Degree of Dissociation

The dissociated species of a typical amino acid HOOC-R-NH<sub>2</sub> in aqueous solution exist in equilibrium as follows<sup>12</sup>:



where R represents the undissociated species, and R<sup>+</sup>, R<sup>-</sup>, and R<sup>±</sup> represent the indicated dissociated species; and,  $K_A$ ,  $K_B$ ,  $K_C$ , and  $K_D$  are the equilibrium constants between R<sup>+</sup> and R<sup>±</sup>, R<sup>+</sup> and R, R<sup>±</sup> and R<sup>-</sup>, and R and R<sup>-</sup>, respectively. The experimentally determined equilibrium constants are  $K_1$ ,  $K_2$ , and  $K_E$ , defined as follows:

$$K_1 = \frac{(\text{H}^+) [(R^\pm) + (R)]}{(R^+)} \quad (5)$$

$$K_2 = \frac{(\text{H}^+) (R^-)}{(R^\pm) + (R)} \quad (6)$$

$$K_E \approx K_B = \frac{(\text{H}^+) (R)}{(R^+)} \quad (7)$$

When the amino acid is completely dissociated,  $(R) = 0$ , and eqs. (5) and (6) reduce to

$$K_1 = \frac{(H^+) (R^\pm)}{(R^+)} \quad (8)$$

$$K_2 = \frac{(H^+) (R^-)}{(R^\pm)} \quad (9)$$

and  $K_1$  and  $K_2$  represent the dissociation constants for  $-\text{COOH}$  and  $-\text{NH}_2$ , respectively. The values of  $K_1$ ,  $K_2$ , and  $K_E$  available in the literature<sup>12,13</sup> for the amino acids studied in this work are listed in Table I.

Let the total concentration of the amino acid in aqueous solution be  $(R_A)$  so that

$$(R_A) = (R) + (R^+) + (R^-) + (R^\pm). \quad (10)$$

From eqs. 5, 6, 7, and 10, the following relations can be derived:

$$\frac{(R)}{(R_A)} = 1 / \left[ \frac{K_1}{K_E} + \frac{(H^+)}{K_E} + \frac{K_1 K_2}{K_E (H^+)} \right] \quad (11)$$

$$\frac{(R^+)}{(R_A)} = \frac{(H^+)}{K_E} / \left[ \frac{K_1}{K_E} + \frac{(H^+)}{K_E} + \frac{K_1 K_2}{K_E (H^+)} \right] \quad (12)$$

$$\frac{(R^-)}{(R_A)} = \frac{K_1 K_2}{K_E (H^+)} / \left[ \frac{K_1}{K_E} + \frac{(H^+)}{K_E} + \frac{K_1 K_2}{K_E (H^+)} \right] \quad (13)$$

$$\frac{(R^\pm)}{(R_A)} = \frac{K_1 - K_E}{K_E} / \left[ \frac{K_1}{K_E} + \frac{(H^+)}{K_E} + \frac{K_1 K_2}{K_E (H^+)} \right]. \quad (14)$$

Equations (11) to (14) represent the fractions of the total concentration of the acid present as undissociated, positively charged, negatively charged, and dipolar species, respectively, in solution, and each of these fractions can be calculated from data on  $K_1$ ,  $K_2$ ,  $K_E$ , and the pH of the solution. There are six aliphatic amino acids (solute numbers 1, 2, 4, 19, 20, and 21) and two aromatic amino acids (solute numbers 24 and 25) in Table I, for which data on  $pK_1$ ,  $pK_2$ , and  $pK_E$  are available. For these acids, the values of  $(R)/(R_A)$ ,  $(R^+)/(R_A)$ ,  $(R^-)/(R_A)$ , and  $(R^\pm)/(R_A)$  have been calculated for the pH values of the acid used in this work, and the results obtained are given in Table III.

### Separation of Aliphatic Amino Acids in Aqueous Solutions

#### *Correlations of Polar Parameters $pK_1$ and $pK_2$ with Data on Membrane Performance*

Figure 1 gives the correlations of  $pK_1$  of acid versus product rate, solute separation, and  $D_{AM}/K\delta$  data obtained at 250 psig with films 5 and 6 (specified in Table II) for aqueous feed solutions involving amino acids 1 to 12 and 14 to 22 listed in Table I. Figure 2 gives the correlation of the

TABLE III  
Data on pH and Degree of Dissociation of Some Amino Acids and Their Hydrochlorides

Solute 1		2	4	19	20	21	24	25
Glycine	DL-Alanine	DL-Leucine	$\beta$ -Alanine	$\gamma$ -Amino- <i>n</i> -butyric acid	$\epsilon$ -Amino- <i>n</i> -caproic acid	<i>m</i> -Amino-benzoic acid	<i>p</i> -Amino-benzoic acid	
pH	6.48	5.75	6.15	5.99	5.84	4.15	4.05	
(R)/(R <sub>A</sub> )	~0	~0	~0	~0	~0	0.231	0.755	
(R <sup>+</sup> )/(R <sub>A</sub> )	~0	~0	0.003	0.017	0.037	0.059	0.016	
(R <sup>-</sup> )/(R <sub>A</sub> )	~0	~0	~0	~0	~0	0.175	0.117	
(R <sup>±</sup> )/(R <sub>A</sub> )	0.999	0.999	0.997	0.983	0.963	0.534	0.112	
			Amino Acid Hydrochloride <sup>a</sup>					
pH	3.06	3.25	3.36	3.57	3.83	3.34	3.10	
(R)/(R <sub>A</sub> )	~0	~0	~0	~0	~0	0.197	0.738	
(R <sup>+</sup> )/(R <sub>A</sub> )	0.186	0.176	0.635	0.820	0.799	0.326	0.141	
(R <sup>-</sup> )/(R <sub>A</sub> )	~0	~0	~0	~0	~0	0.023	0.013	
(R <sup>±</sup> )/(R <sub>A</sub> )	0.814	0.824	0.365	0.180	0.201	0.454	0.109	

<sup>a</sup> Aqueous solutions of amino acids with equimolal quantities of HCl.



same solute separation data versus the corresponding  $pK_2$  of the acids. The 21 amino acids involved in these correlations cover a  $pK_1$  range of 1.71 to 4.43 and a  $pK_2$  range of 8.33 to 10.75; the pH range involved in the aqueous feed solutions used is 5.75 to 6.48. The data on pH (Table III) were obtained by direct measurement. On the basis of the data given in Table III, one may conclude that, in the aqueous feed solutions used, all the above amino acids were essentially completely dissociated (and hence  $pK_1$  and  $pK_2$  referred essentially to the acidity of the carboxylate anion and amino cation, respectively), and more than 96% of the dissociated species was in the form of zwitter ions,  $R^\pm$ .

The sodium chloride separations for films 5 and 6 at 250 psig were 70.6% and 58.3%, respectively. Figure 1 shows that amino acids were better separated than sodium chloride in all the cases tested, which means that the critical pore diameter for the separation of amino acid ions is generally higher than that for the separation of sodium chloride.

Figure 1 shows that the product rates remained essentially constant with respect to each film in all cases, which indicates that the porous structure of the film surface was not affected during these experiments.

With respect to each film, the solute separation data varied only within a narrow range in the entire region of  $pK_1$  values involved. However, the correlations are significant in some important respects. First, the correlations are similar for both the films tested, indicating the generality of the form of such correlations. Secondly, solute separation passed through a minimum at  $pK_1$  value of  $\sim 4.0$ . The same observation was made earlier<sup>3</sup> with respect to the separation of monocarboxylic acids using the same type of membranes. This observation confirms the existence of minimum separation in reverse osmosis with change in acidity of the carboxylate ion. This observation also focuses attention on the general problem of establishing physicochemical criteria for the differences in the separation of different anions and cations (both organic and inorganic) in reverse osmosis. Finally, in the narrow range of  $pK_1$  values 2.2 to 2.4, the solute separation data are highly scattered indicating the simultaneous effect of another factor governing reverse osmosis separation. In the above  $pK_1$  range, there are ten amino acids involved (solutes 1 to 5, 15 to 18, and 22 in Table I). On the basis of the earlier work on polar and steric effects on reverse osmosis,<sup>14</sup> it is reasonable to expect that the scatter in solute separation in Figure 1 is probably due to steric effect. This aspect of the subject is explored below in detail.

It may be pointed out here that solute separation is not a constant quantity; it varies depending on the mass transfer coefficient  $k$  on the high-pressure side of the membrane. The data on solute separation given in Figure 1 are for the values of  $k$  given in Table I. If  $k$  changes, solute separation will also change. For example, for the values of  $k$  used in these experiments, the data on solute separation shown in Figure 1 are in the range of 80% to 88% for film 5 and 67% to 79% for film 6; when  $k = \infty$  (i.e., under conditions of no concentration polarization), solute separation data

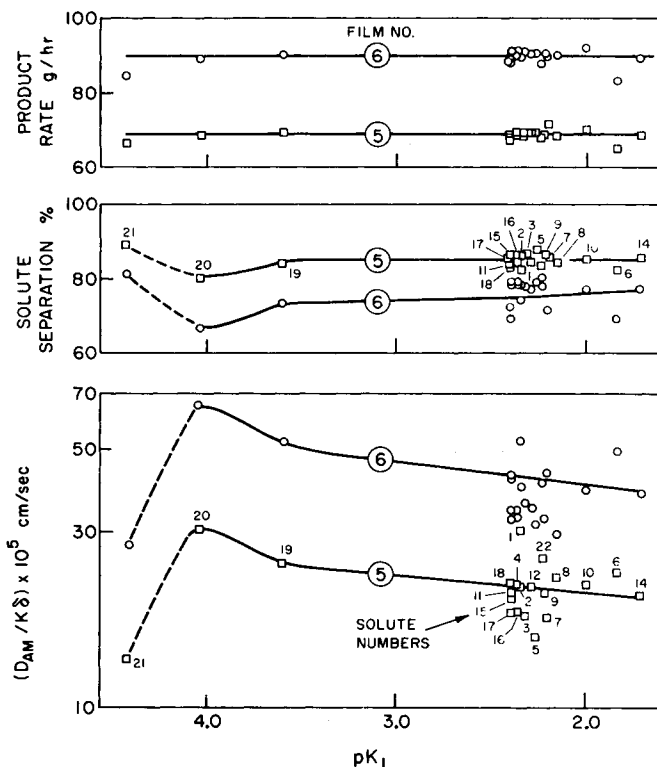


Fig. 1. Correlations of  $pK_1$  of amino acids vs. product rate, solute separation, and solute transport parameter. Film type, cellulose acetate, Batch 316 (10/30); operating pressure, 250 psig; feed concentration, 0.001–0.003 g-mole/l.; feed flow rate, 400 cc/min; membrane area, 7.6 cm<sup>2</sup>; solute numbers, same as in Table I.

may be calculated from eq. (4) to be in the range of 89% to 94% for film 5 and 83% to 91% for film 6. Consequently, for the values of  $k$  between those given in Table I and  $\infty$ , solute separations can change in the range of 80% to 94% for film 5 and 67% to 91% for film 6; the ranges will be even wider if values of  $k$  lower than those given in Table I are considered. Therefore, even though solute separation data given in Figure 1 seem to vary in a narrow range at the arbitrary values of  $k$  chosen for experiments, the above data cannot be considered to represent essentially constant solute separation for all solutes for all values of  $k$ . Similar comments also apply to solute separation data in Figures 2, 4, 7, and 10. The data on solute separation are, however, easy to visualize, and they can help in identifying the existence (or otherwise) of possible correlations if only the experimental conditions used for the different solution systems are comparable. Since such is the case in this work, correlations of data on solute separation given in Figures 1, 2, 4, 7, and 10 are useful.

On the other hand, solute transport parameter  $D_{AM}/K\delta$  is independent of  $k$ . Therefore, correlations based on data on  $D_{AM}/K\delta$  have firm significance.

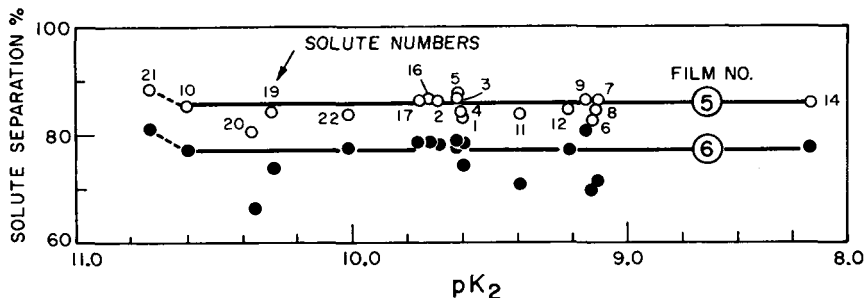


Fig. 2. Correlation of  $pK_2$  of amino acids vs. solute separation. Film type, cellulose acetate, Batch 316 (10/30); operating pressure, 250 psig; feed concentration, 0.001–0.003 g-mole/l.; feed flow rate, 400 cc/min; membrane area, 7.6 cm<sup>2</sup>; solute numbers, same as in Table I.

Referring to Figure 1 again, the data show that the  $D_{AM}/K\delta$ -versus- $pK_1$  correlations are similar for both films, the change in  $D_{AM}/K\delta$  with change in  $pK_1$  is more explicit, and there is considerable scatter of  $D_{AM}/K\delta$  data in the narrow  $pK_1$  range of 2.2 to 2.4. In view of both the theoretical and practical importance of the  $D_{AM}/K\delta$  data, the above correlations will be considered in more detail a little later in this discussion.

The correlations of solute separation data versus  $pK_2$  values shown in Figure 2 do not indicate any definite variations. Solute separations were relatively insensitive to change in  $pK_2$  values for the amino acids used. This conclusion was supported by the data on separations of the hydrochlorides of benzylamine ( $pK_a = 9.34$ ), trimethylamine ( $pK_a = 9.76$ ), and dimethylamine ( $pK_a = 10.87$ ); under the same experimental conditions used for amino acid separations, solute separations for the above hydrochlorides were 73.4%, 76.1%, and 75.3%, respectively, with film 5. The latter data show that differences in the separations of completely ionized amines are not significant when the basicity of the amines are less than that represented by  $pK_a = 10.87$ .

On the basis of the foregoing results, one may conclude that the cellulose acetate membrane material used in this work is more sensitive to the acidity of the carboxyl group than that of amino group, and  $pK_1$  is a more relevant polar parameter than  $pK_2$  for purposes of correlation of reverse osmosis separation data for the above amino acids.

#### *Correlation of Data on Amino Acid Separations with Those on Steric Parameter*

The earlier work on polar and steric effects in reverse osmosis<sup>14</sup> is the starting point for this part of the study. In order to investigate the influence of steric effect on reverse osmosis separations of amino acids, it is first necessary to obtain numerical data on the steric parameter  $\Sigma E_s$ , applicable for amino acids. Such data are not directly available in the literature. Therefore, an empirical method of generating such data from the ex-

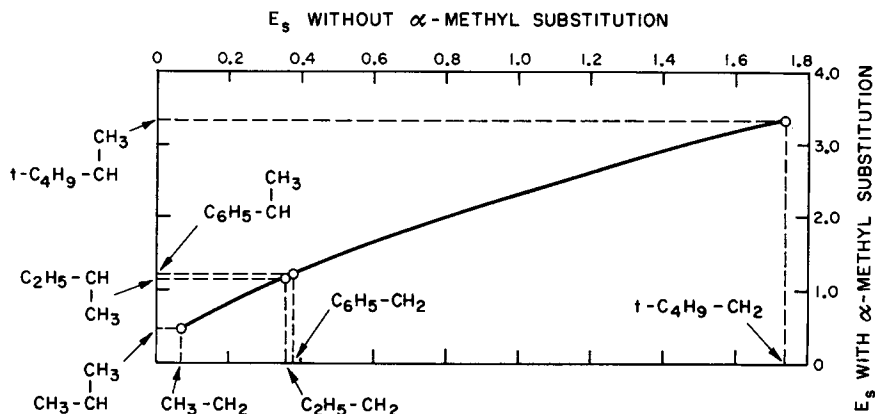


Fig. 3. Correlation of  $E_s$  without methyl substitution in the  $\alpha$ -position vs.  $E_s$  with methyl substitution in the  $\alpha$ -position.

perimental data available in the literature<sup>15,16</sup> was developed. The details of this method are as follows.

Figure 3 is a correlation of  $E_s$  values taken from Taft table<sup>15</sup> for  $\text{CH}_3\text{CH}_2$  versus  $\text{CH}_3\text{CH}_3\text{CH}$ ,  $\text{C}_2\text{H}_5\text{CH}_2$  versus  $\text{C}_2\text{H}_5\text{CH}_3\text{CH}$ ,  $\text{C}_6\text{H}_5\text{CH}_2$  versus  $\text{C}_6\text{H}_5\text{CH}_3\text{CH}$ , and  $t\text{-C}_4\text{H}_9\text{CH}_2$  versus  $t\text{-C}_4\text{H}_9\text{CH}_3\text{CH}$ . This correlation shows the change in the numerical value of  $E_s$  as a result of substitution of  $\text{CH}_3$  in the  $\alpha$ -position. Wherever applicable, this correlation can be used for the estimation of  $\Sigma E_s$  values.

An amino acid containing a single  $-\text{COOH}$  and a single  $-\text{NH}_2$  group is treated as a monocarboxylic acid whose hydrocarbon side chain includes a substitution by an amino group. It is assumed that the steric effects due to the amino substituent groups  $-\text{NH}_2$ ,  $-\text{NH}-$ , and  $(\text{CH}_3)_3\text{N}^+$  are the same as those due to the hydrocarbon substituent groups  $-\text{CH}_3$ ,  $-\text{CH}_2-$ , and  $(\text{CH}_3)_3\text{C}-$ , respectively. On this basis, the  $\Sigma E_s$  value for an amino acid is obtained by one of the following means: (i) replace the amino group by the equivalent hydrocarbon group and find the  $\Sigma E_s$  value for the resulting hydrocarbon substituent group in the corresponding monocarboxylic acid; or (ii) replace the original  $\text{NH}_2-$  group by  $\text{H}$ ; find the  $\Sigma E_s$  value for the resulting hydrocarbon substituent; then use Figure 3 to obtain the final  $\Sigma E_s$  value resulting from  $-\text{CH}_3$  substitution in the  $\alpha$ -position. This procedure is described below in detail with respect to each one of the amino acids whose  $\Sigma E_s$  value was used in this work. The number on the left of each compound is the solute number in Table I; unless otherwise stated, the  $E_s$  values used are those taken from Taft table<sup>15</sup>:

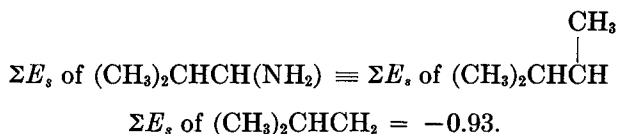
1. Glycine

$$\Sigma E_s \text{ of } \text{CH}_2(\text{NH}_2) \equiv \Sigma E_s \text{ of } \text{CH}_2\text{CH}_3 = -0.07.$$

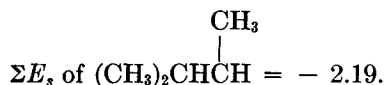
2. DL-Alanine

$$\Sigma E_s \text{ of } \text{CH}_3\text{CH}(\text{NH}_2) \equiv \Sigma E_s \text{ of } \text{CH}_3\text{CHCH}_3 = -0.47.$$

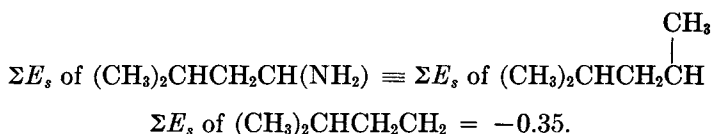
## 3. DL-Valine



Therefore, from Figure 3,



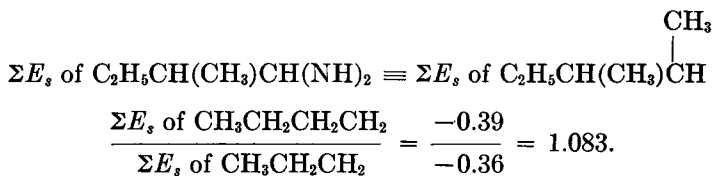
## 4. DL-Leucine



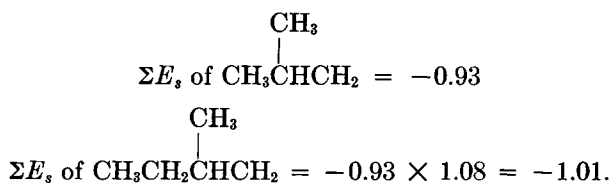
From Figure 3,



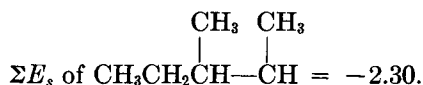
## 5. DL-Isoleucine



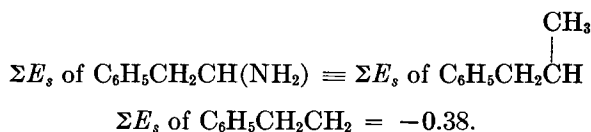
This shows that the substitution of H by  $\text{CH}_3$  increases the magnitude of  $\Sigma E_s$  by a factor of 1.083. Since



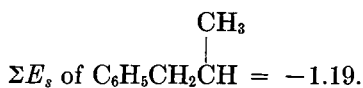
From Figure 3,



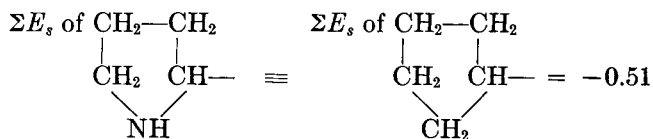
## 6. DL-Phenylalanine



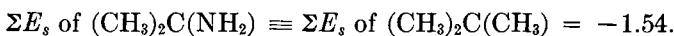
From Figure 3,



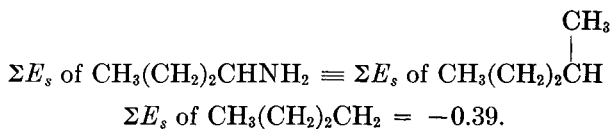
10. L-Proline



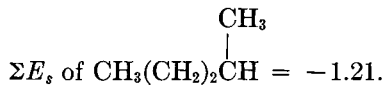
15.  $\alpha$ -Aminoisobutyric Acid



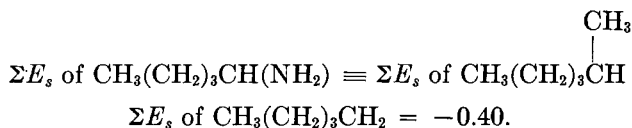
16. DL-Norvaline



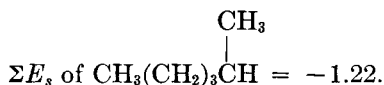
From Figure 3,



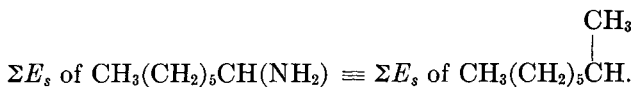
17. DL-Norleucine



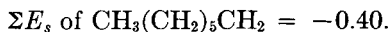
From Figure 3,



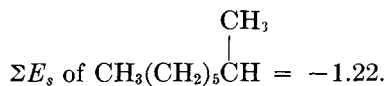
18. DL- $\alpha$ -Aminocaprylic Acid



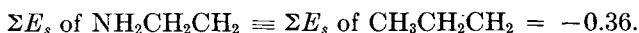
From reference 16,



From Figure 3,



19.  $\beta$ -Alanine



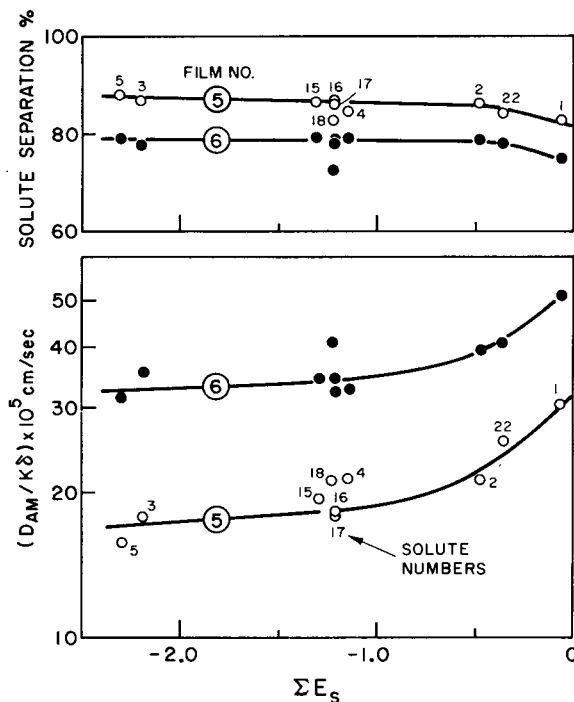


Fig. 4. Correlation of  $\Sigma E_s$  of amino acids vs. solute separation and solute transport parameter. Film type, cellulose acetate, Batch 316 (10/30); operating pressure, 250 psig; feed concentration, 0.001–0.003 g-mole/l.; feed flow rate, 400 cm/min; membrane area, 7.6 cm<sup>2</sup>; solute numbers, same as in Table I.

20.  $\gamma$ -Amino-*n*-butyric Acid

$$\Sigma E_s \text{ of } \text{NH}_2\text{CH}_2\text{CH}_2\text{CH}_2 \equiv \Sigma E_s \text{ of } \text{CH}_3\text{CH}_2\text{CH}_2\text{CH}_2 = -0.39.$$

21.  $\epsilon$ -Amino-*n*-caproic Acid

$$\Sigma E_s \text{ of } \text{NH}_2(\text{CH}_2)_5 \equiv \Sigma E_s \text{ of } \text{CH}_3(\text{CH}_2)_5 = -0.40.$$

from reference 16.

22. Sarcosine

$$\Sigma E_s \text{ of } \text{CH}_3\text{NHCH}_2 \equiv \Sigma E_s \text{ of } \text{CH}_3\text{CH}_2\text{CH}_2 = -0.36.$$

23. Betaine

$$\Sigma E_s \text{ of } (\text{CH}_3)_3\text{NCH}_2 \equiv \Sigma E_s \text{ of } (\text{CH}_3)_3\text{CCH}_2 = -1.74.$$

Figure 4 illustrates the correlations of  $\Sigma E_s$  values (estimated by the procedure outlined above) and data on solute separation and  $D_{AM}/K\delta$  for the ten solutes referred earlier in the  $pK_1$  range of 2.2 to 2.4. While the same separation data and  $D_{AM}/K\delta$  data appear scattered in Figure 1, such scatter has virtually disappeared in the correlations shown in Figure 4. Further, Figure 4 shows that as the  $\Sigma E_s$  value increases (representing a decrease in steric effect),  $D_{AM}/K\delta$  tends to increase and consequently solute

separation tends to decrease, just as observed earlier in the study of ether solutes.<sup>14</sup> These results indicate that the reverse osmosis separation of amino acids is controlled both by the polar and steric character of the solute molecules.

*Results of Regression Analysis and Predictability of  
Membrane Performance*

On the basis of the foregoing conclusion, the possibility of expressing solute transport parameter  $D_{AM}/K\delta$  as a function of polar and steric parameters representing the solute was next investigated. For this purpose the data on  $pK_1$  and  $\Sigma E_s$  as estimated above were taken as the relevant polar and steric parameters, respectively. Following previous work,<sup>14</sup>  $D_{AM}/K\delta$  could be expressed as

$$D_{AM}/K\delta = C^* \exp(\rho^* pK_1 + \delta^* \Sigma E_s) \quad (15)$$

where  $\rho^*$  and  $\delta^*$  are the polar and steric coefficients, respectively, and  $C^*$  is a proportionality factor depending on the porous structure of the membrane surface. Figure 1 shows that  $D_{AM}/K\delta$  passes through a maximum at  $pK_1 \cong 4.0$ . While the general form of eq. (15) may be expected to be valid for the entire range of  $pK_1$  values, the numerical values of  $C^*$ ,  $\rho^*$ , and  $\delta^*$  may be expected to be unique for the two ranges of  $pK_1$  values on either side of the maximum  $D_{AM}/K\delta$ . Since, in this work, sufficient experimental data are available only for the range of  $pK_1$  values less than 4.03, the applicability of eq. (15) could be investigated only for the latter set of data.

In the range of  $pK_1$  values of 4.03 or less, the  $D_{AM}/K\delta$  data for 20 amino acids are included in Figure 1; but, values of  $\Sigma E_s$  have been estimated only for 14 of the above acids. The remaining six acids (solutes 7 to 9, 11, 12, and 14 in Table I) have additional polar groups or complicated structures, and a method of estimating  $\Sigma E_s$  for such compounds has not yet been established. Consequently, the applicability of eq. (15) was investigated with  $D_{AM}/K\delta$  data on solutes 1 to 6, 10, 15 to 20, and 22 listed in Table I.

The  $D_{AM}/K\delta$  data obtained with film 5 for the 14 solutes referred above were subjected to multiple regression analysis for linear correlation<sup>17</sup> in terms of eq. 15. This analysis, represented in Figure 5, gave the following results for film 5:  $\rho^* = 0.071$ ,  $\delta^* = 0.216$ , and  $\ln C^* = -8.39$ . The values of the coefficients of determination  $R_{pK_1}^2$  and  $R_{\Sigma E_s}^2$  obtained were 0.102 and 0.637, respectively, indicating that the contribution of  $pK_1$  to  $\ln(D_{AM}/K\delta)$  is relatively small compared to that of  $\Sigma E_s$ . It may be recalled that each of the values of  $R_{pK_1}^2$  and  $R_{\Sigma E_s}^2$  represents the fraction of total variance of the dependent variable  $\ln(D_{AM}/K\delta)$  which is related respectively to the particular factor  $pK_1$  or  $\Sigma E_s$  considered.

The summation of  $R_{pK_1}^2$  and  $R_{\Sigma E_s}^2$  values given above (= 0.739) is rather low compared to 1.0. This indicates that either eq. (15) is an inadequate representation of data, or the relative variation in the dependent variable is too much compared to the total variation involved in the range of data analyzed. The latter is indeed the case here, because the solute



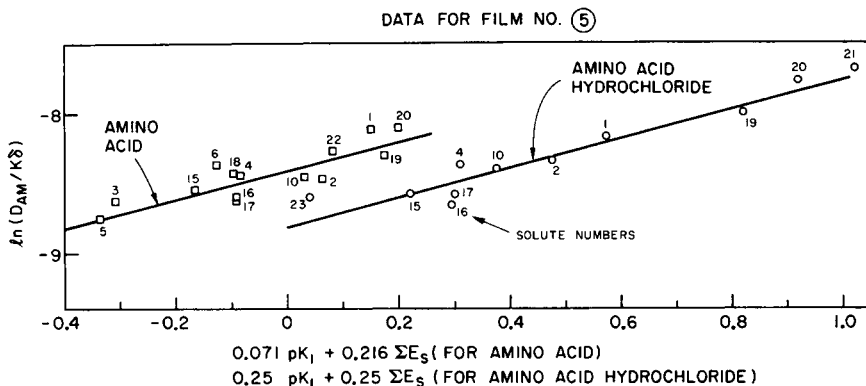


Fig. 5. Correlation of  $(\rho^* \Sigma \sigma^* + \delta^* \Sigma E_s)$  vs.  $\ln(D_{AM}/K\delta)$  for amino acids and amino acid hydrochlorides. Film type, cellulose acetate, Batch 316 (10/30); operating pressure, 250 psig; feed concentration, 0.001–0.003 g-mole/l.; flow rate, 400 cc/min; membrane area, 7.6 cm<sup>2</sup>; solute numbers, same as in Table I.

separations for the systems considered varied in the narrow range of 80% to 88% with a  $\pm 2\%$  experimental error.

The adequacy of eq. (15) to represent the experimental solute separation data in the  $pK_1$  range of 4.03 to 1.71 was tested by three sets of calculations involving films 2, 5, and 6. It may be noted that the average size of pores on the membrane surface (as represented by their  $D_{AM}/K\delta$  data for sodium chloride given in Table II) is smaller for film 2 and higher for film 6 compared to that for film 5.

In the first set of calculations, the values of  $D_{AM}/K\delta$  for all the 14 amino acids referred earlier were calculated for film 5 using eq. (15) and the  $\rho^*$ ,  $\delta^*$ , and  $\ln C^*$  values obtained above by regression analysis for linear correlation. Using these values of  $D_{AM}/K\delta$  and the values of  $k$  given in Table I, solute separation  $f$  for each amino acid was determined using eq. (4) in which  $PWP$  is approximated as  $PR$ . The data on solute separation so determined were compared with the corresponding experimental values. The results, plotted in Figure 6, showed that the experimental and calculated values were in good agreement in all cases.

The purpose of the calculations with respect to films 2 and 6 was to test the adequacy of eq. (15) to predict solute separation for other films. In these calculations, the values of  $\rho^*$  and  $\delta^*$  used for film 5 were assumed valid for films 2 and 6 also. Experimental  $D_{AM}/K\delta$  values for a reference solute were used to obtain  $\ln C^*$  values for each film using eq. (5). Choosing for illustration DL-isoleucine (solute 5 in Table I) as the reference solute, the values of  $\ln C^*$  obtained for films 2 and 6 were  $-10.45$  and  $-7.73$ , respectively. Using the respective  $\ln C^*$  values for films 2 and 6, and the same  $\rho^*$  ( $= 0.071$ ),  $\delta^*$  ( $= 0.216$ ), and the  $k$  values (given in Table I) for both the films, the values of  $D_{AM}/K\delta$  for each of the other 13 solutes under study were calculated, and the corresponding solute separations obtainable were predicted using eq. (4) as before. The data on solute separations so

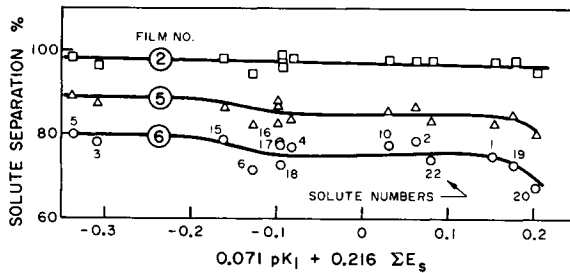


Fig. 6. Effect of  $(\rho^*\Sigma\sigma^* + \delta^*\Sigma E_s)$  on solute separation of amino acids for films 2, 5, and 6: (—) predicted; ( $\square$ ,  $\Delta$ ,  $\circ$ ) experimental. Film type, cellulose acetate, Batch 316 (10/30); operating pressure, 250 psig; feed concentration, 0.001–0.003 g-mole/l.; flow rate, 400 cc/min; membrane area, 7.6 cm<sup>2</sup>; solute numbers, same as in Table I.

predicted were then compared with those obtained experimentally. The results (also plotted in Fig. 6) showed that the experimental and calculated values were again in good agreement in all cases.

From the foregoing results, one may draw the following conclusions with reference to completely ionized amino acids discussed above in the  $pK_1$  range of 4.03 to 1.71: (i)  $pK_1$  expresses the polar character of the solute adequately for purposes of correlation of data on membrane performance; (ii) the method outlined above for estimating the steric parameter  $\Sigma E_s$  is valid for practical purposes of predicting membrane performance; (iii) the solute transport parameter is a function of both  $pK_1$  and  $\Sigma E_s$ , with the latter parameter having a relatively greater influence; (iv) eq. (15) is a valid quantitative expression for the solute transport parameter; and (v) for purposes of predicting membrane performance, the numerical values of the polar coefficient  $\rho^*$  and steric coefficient  $\delta^*$  may be taken to be 0.071 and 0.216, respectively, for the type of cellulose acetate membrane material used in this work; the above values of  $\rho^*$  and  $\delta^*$  may be assumed independent of the pore structure on the membrane surface.

## Separation of Aliphatic Amino Acid Hydrochlorides in Aqueous Solutions

### *Correlation of Data on Membrane Performance with $pK_1$ of Acid*

As pointed out already, the aliphatic amino acids studied above were essentially completely dissociated in aqueous solutions, and the dissociated species existed mostly in the form of  $R^\pm$ . The dissociation equilibrium could however be shifted, and the equilibrium concentration of  $R^+$  or  $R^-$  could be consequently increased by decreasing or increasing respectively the pH of the aqueous solution. The object of this part of the study was to investigate the effect of such increase in equilibrium concentration, on overall separation of amino acid in reverse osmosis. In view of the susceptibility of the membrane material for alkaline hydrolysis, this study was limited to the study of the effect of increasing the equilibrium concentration of  $R^+$  by acidifying the aqueous solution of the amino acid.

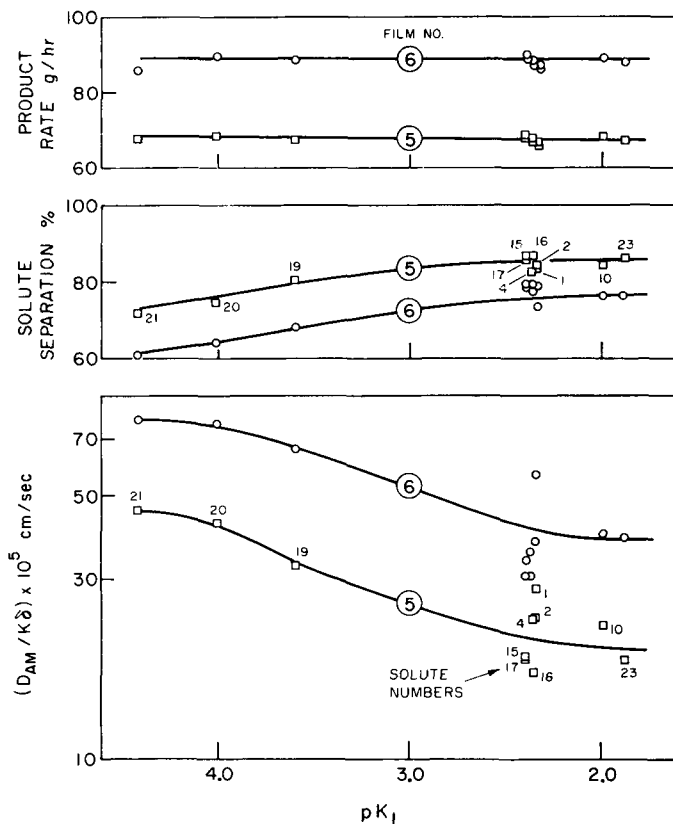


Fig. 7. Correlations of  $pK_1$  of amino acid hydrochlorides vs. product rate, solute separation, and solute transport parameter. Film type, cellulose acetate, Batch 316 (10/30); operating pressure, 250 psig; feed concentration, 0.001–0.003 g-mole/l.; flow rate, 400 cc/min; membrane area, 7.6 cm<sup>2</sup>; solute numbers, same as in Table I.

For the purpose of this study, 11 amino acids (solutes 1, 2, 4, 10, 15, 16, 17, 19, 20, 21, and 23 listed in Table I, for which  $\Sigma E_s$  values are available and which contain no additional polar group other than one  $-\text{NH}_2$  and one  $-\text{COOH}$ ) were chosen for illustration. Equimolar quantities of amino acid and hydrochloric acid were used in aqueous feed solution. The effect of addition of HCl was to decrease the pH and shift the dissociation equilibrium in the direction of higher concentration of  $\text{R}^+$ . This is quantitatively illustrated in Table III for the case of glycine, DL-alanine, DL-leucine,  $\beta$ -alanine,  $\gamma$ -amino-*n*-butyric acid, and  $\epsilon$ -amino caproic acid (solutes 1, 2, 4, 19, 20, and 21, respectively, in Table I) for which data on  $pK_1$ ,  $pK_2$ , and  $pK_E$  are available.

Figure 7 gives the correlations of  $pK_1$  of acid versus product rate, solute separation, and  $D_{AM}/K\delta$  data obtained at 250 psig with films 5 and 6 for the above aqueous amino acid hydrochloride solutions. These correlations are interesting from several points of view.

Figure 7 shows that the product rates remained essentially constant with respect to each film in all the cases studied, which indicates that the porous structure of the film surface was not affected during the experiments even though the pH of the feed solutions used was in the range 2.95 to 3.83. This is not surprising since cellulose acetate membranes have been shown to exhibit stable reverse osmosis performance even after exposure to pH = 3 for one year.<sup>18</sup>

The solute separation-versus- $pK_1$  correlation is comparable to that shown in Figure 1. With amino acid hydrochloride feed solutions, Figure 7 shows that solute separation tends to increase with decrease in  $pK_1$  in the entire range of  $pK_1$  values (4.43 to 1.71) studied. In particular, no minima in solute separation was observed in the above  $pK_1$  range. This shows that, for amino acid hydrochloride feed solutions, the minimum in solute separation, if it does exist, is shifted in the direction of higher  $pK_1$  value.

The cellulose acetate membrane material has already been shown to exhibit a net proton acceptor character.<sup>2</sup> This means that, at the membrane-solution interface, solute repulsion is more for an anion than for a cation. Consequently, with increase in the concentration of  $R^+$ , and the corresponding decrease in that of  $R^\pm$ , one should expect the overall solute separation to decrease. Since the above concentration change is also associated with increase in  $pK_1$  (see Tables I and III), overall solute separations must be lower for amino acid hydrochloride solutions than for amino acid solutions especially in the higher range of  $pK_1$  values. This is explicitly illustrated by the experimental data for  $\beta$ -alanine,  $\gamma$ -amino-*n*-butyric acid, and  $\epsilon$ -amino-*n*-caproic acid (solutes 19, 20, and 21) shown in Figures 1 and 7.

As in Figure 1, solute separation data in Figure 7 are scattered in the  $pK_1$  range of 2.2 to 2.4; this scatter is again understandable on the basis of steric effects.

As stated earlier with reference to Figure 1, the correlations of data on  $D_{AM}/K\delta$  with  $pK_1$  are even more important. Figure 7 shows that  $D_{AM}/K\delta$  decreases significantly with decrease in  $pK_1$ , and there is again considerable scatter of  $D_{AM}/K\delta$  data in the  $pK_1$  range of 2.2 to 2.4. These correlations are discussed below in detail.

#### *Results of Regression Analysis and Predictability of Membrane Performance*

The  $D_{AM}/K\delta$  data obtained with film 5 for the 11 amino acid hydrochloride feed solutions referred above were subjected to multiple regression analysis for linear correlation in terms of eq. (15) as before. This analysis, also represented in Figure 5, gave the following results for film 5:  $\rho^* = 0.25$ ,  $\delta^* = 0.25$ , and  $\ln C^* = -8.78$ . The values for the coefficient of determination  $R_{pK_1}^2$  and  $R_{\Sigma E_i}^2$  obtained were 0.499 and 0.382, respectively, so that this sum  $R_{pK_1}^2 + R_{\Sigma E_i}^2 = 0.881$ .

The adequacy of eq. (15) to represent the experimental solute separation data for the amino acid hydrochlorides in the  $pK_1$  range of 4.43 to 1.71 was

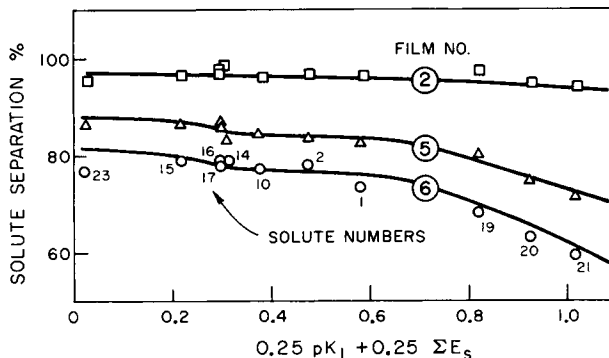


Fig. 8. Effect of  $(\rho^*\Sigma\sigma^* + \delta^*\Sigma E_s)$  on solute separation of amino acid hydrochlorides for films 2, 5, and 6. (—) predicted; ( $\square$ ,  $\Delta$ ,  $\circ$ ) experimental. Film type, cellulose acetate, Batch 316 (10/30); operating pressure, 250 psig; feed concentration, 0.001–0.003 g-mole/l.; flow rate, 400 cc/min; membrane area, 7.6 cm<sup>2</sup>; solute numbers, same as in Table I.

tested by back calculating solute separations for films 2, 5, and 6. The procedure used for these calculations was exactly the same as that used before for unacidified amino acid feed solutions (Fig. 6). The same values of  $\rho^*$  ( $=0.25$ ) and  $\delta^*$  ( $=0.25$ ) were used for all the three films. The  $\ln C^*$  values for films 2 and 6 were obtained from the experimental  $D_{AM}/K\delta$  data for the hydrochloride of  $\alpha$ -aminoisobutyric acid (reference solute); the values of  $\ln C^*$  so obtained were  $-10.77$  and  $-8.21$  for films 2 and 6, respectively. The values of  $k$  listed in Table I were used for all the three films. Both the experimental and calculated solute separation data are plotted in Figure 8 which shows excellent agreement between the two sets of data for each of the films tested.

The foregoing results show that eq. (15) adequately represents the  $D_{AM}/K\delta$  data for aqueous feed solutions of equimolar quantities of amino acid and hydrochloric acid, in the  $pK_1$  range of 4.43 to 1.71. For such feed solutions, a  $\rho^*$  value of 0.25 and a  $\delta^*$  value of 0.25 can be used for purposes of predicting membrane performance with the type of cellulose acetate membranes used in this work. Further, the above values of  $\rho^*$  and  $\delta^*$  may be considered independent of the porous structure of the membrane surface.

Comparing the numerical values of  $\rho^*$ ,  $\delta^*$ , and the sum  $R_{pK_1}^2 + R_{\Sigma E_s}^2$  obtained with film 5 for the amino acid hydrochloride systems discussed above and the amino acid systems discussed earlier, the following observations are significant. The value of  $\rho^*$  is about  $3\frac{1}{2}$  times higher for the former systems, and the values of  $\delta^*$  are about the same for both the systems. This means that the effect of increasing the concentration of  $R^+$  in the feed solution is to increase the value of  $\rho^*$  and decrease overall solute separation with increase in  $\rho^*pK_1 + \delta^*\Sigma E_s$ . The latter effect is illustrated by the data in Figure 8. The reason for this effect is understandable on the basis of the net basic (proton acceptor) character of the cellulose acetate

membrane material. The absence of any significant difference in the values of  $\delta^*$  for the two types of feed solutions indicates the absence of any significant difference in the steric effects of  $R^+$  and  $R^\pm$ . The sum of the values of the coefficients of determination is close to one for the amino acid hydrochloride systems than for the amino acid systems. This is understandable on the basis of the wider range of solute separation data involved in the former case with the same range of experimental error in both cases.

### Effect of pH on Separation of $\beta$ -Alanine

A set of experiments were carried out with aqueous solutions of  $\beta$ -alanine to study the effect of pH of feed solution on overall solute separation in reverse osmosis. Two new film samples (films 7 and 8) were used for this study. The aqueous solution of  $\beta$ -alanine had a pH of 6.15; different quantities of HCl or NaOH were added to this solution to decrease or increase the pH of the feed solution. Five feed solutions of pH 3.60, 4.10, 6.15, 9.99, and 10.24 were tested. The overall solute separation data obtained with the above feed solutions for films 7 and 8 at 500 psig are given in Table IV which shows that, with respect to each film, solute separation increased with increase in pH of the feed solution. These results are consistent with those discussed earlier for amino acid and amino acid hydrochloride feed solutions, and they are explicable on the basis that the net effect of increase in pH of the feed solution is to decrease the equilibrium concentration of  $R^+$  or increase the equilibrium concentration of  $R^-$  in the feed solution. Further, since  $\beta$ -alanine is completely dissociated in the entire pH range studied, the increase in solute separation with increase in pH shows that solute repulsion at the membrane-solution interface, and hence solute separation in reverse osmosis, with respect to each ionic species, is in the order  $R^- > R^\pm > R^+$  for the cellulose acetate membrane material used.

A procedure for predicting quantitatively the effect of pH of feed solution on overall separation of  $\beta$ -alanine in the systems studied above was then in-

TABLE IV  
Effect of pH on Separation of  $\beta$ -Alanine\*

pH	$\rho^*$	$\delta^*$	$\ln C^*$	$\ln D_{AM}/K\delta$	Solute separation, %	
					Calculated	Experimental
Film 7						
3.36	0.253	0.233	-9.283	-8.456	87.1	87.3
4.10	0.205	0.233	-9.179	-8.525	87.9	86.5
6.15	0.071	0.233	-8.891	-8.719	89.8	89.8
9.99	-0.179	0.233	-8.351	-9.079	92.7	92.7
10.24	-0.196	0.233	-8.316	-9.106	92.8	92.1
Film 8						
3.36	0.253	0.233	-9.761	-8.934	91.5	90.7
4.10	0.205	0.233	-9.657	-9.003	92.0	90.7
6.15	0.071	0.233	-9.369	-9.197	93.3	93.3
9.99	-0.179	0.233	-8.829	-9.557	95.2	94.0
10.24	-0.196	0.233	-8.794	-9.584	95.4	94.1

\* Operating pressure: 500 psig.

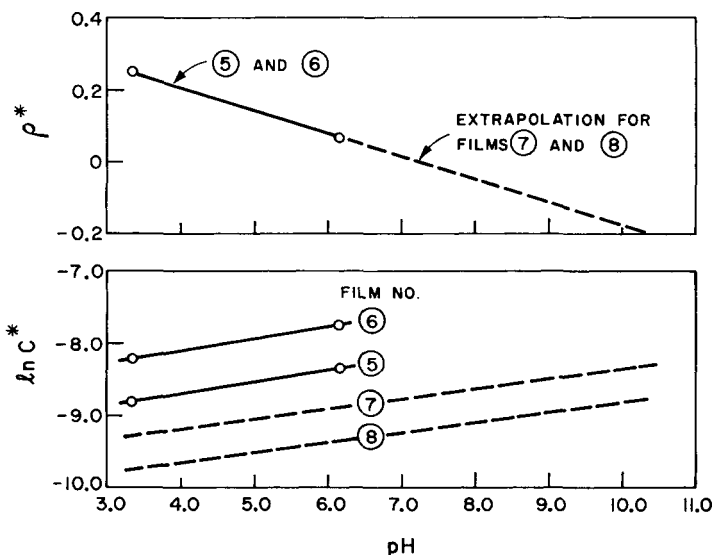


Fig. 9. Effect of pH on  $\rho^*$  and  $\ln C^*$ . Film type, cellulose acetate, Batch 316 (10/30); operating pressure, 250 psig for films 5 and 6 and 500 psig for films 7 and 8; feed concentration, 0.001 g-mole/l.; flow rate, 400 cc/min; membrane area, 7.6 cm<sup>2</sup>; solute,  $\beta$ -alanine.

investigated. This prediction procedure is based on three assumptions: (i) the numerical values of  $\rho^*$  and  $\delta^*$  at 500 psig are the same as those at 250 psig<sup>19</sup>; (ii) the value of  $\rho^*$  decreases linearly with increase in pH of the feed solution; and (iii)  $\ln C^*$  is a linear function of pH of feed solution, and the difference in the values of  $\ln C^*$  per given change in pH is the same for all membranes irrespective of their surface porosities. The latter two assumptions are illustrated in Figure 9 using the data obtained earlier with films 5 and 6 used in conjunction with  $\beta$ -alanine solutions at 250 psig. The experimental values of  $\ln C^*$  plotted in Figure 9 for films 5 and 6 at pH values of 6.15 and 3.36 partially support assumption (iii) above.

Using the above assumptions, the procedure used for predicting solute separations was as follows. Since  $\delta^*$  values of 0.216 and 0.25 were obtained for  $\beta$ -alanine solutions studied earlier, an average value of 0.233 was assumed for all pH values; the value of  $\rho^*$  at the desired pH of feed was obtained by linear interpolation in Figure 9. The same values of  $\delta^*$  and  $\rho^*$  were used for films 7 and 8. Using the experimental data on  $\ln C^*$  for films 7 and 8 for pH 6.15, the applicable value of  $\ln C^*$  at the desired pH was estimated on the basis of assumption (iii) above as indicated in Figure 9. Using the above values of  $\rho^*$ ,  $\delta^*$ , and  $\ln C^*$ , together with the data on  $pK_1$  and  $\Sigma E_s$  for  $\beta$ -alanine given in Table I, the values of  $D_{AM}/K\delta$  at different pH values were calculated using eq. (15). The corresponding solute separation was then calculated, as before, using eq. (4), and the value of  $k$  for  $\beta$ -alanine given in Table I. Data on solute separation thus obtained are also given in Table IV, which shows excellent agreement between calculated and experimental results, suggesting the possible validity of the

assumptions involved and the generality of the prediction procedure outlined above.

### Effect of Additional Polar Substitutions on the Separation of Aliphatic Amino Acids

Among the amino acids 1 to 23 listed in Table I, there are several (solutes 7, 8, 9, 12, 13, and 14) which contain an additional polar group substitution such as —OH, —S, or —SH in their structures. The effect of such substitution on overall solute separation in reverse osmosis can be seen by comparing the relative magnitude of  $D_{AM}/K\delta$  data for the substituted and the corresponding unsubstituted amino acids. For example, the values of  $(D_{AM}/K\delta) \times 10^5$  (cm/sec, given below in brackets) obtained with film 5 at 250 psig, for some comparable solutes show the following order:

$$\text{solute 7 (17.52)} < \text{solute 6 (23.29)}$$

$$\text{solute 9 (20.29)} < \text{solute 14 (20.82)} < \text{solute 2 (21.08)}$$

$$\text{solute 13 (0.10)} < \text{solute 14 (20.82)}.$$

The above orders show that the effect of substitution of additional polar group in the amino acid is to decrease  $D_{AM}/K\delta$  and hence increase solute separation in reverse osmosis. This result is understandable on the basis of previous work on polyhydric alcohols.<sup>8</sup> Substitution of an additional polar group results in more negative Taft number ( $\sigma^*$ ) for the substituent group, which represents increased basicity (proton accepting power) for the molecule. The latter is responsible for increased solute repulsion at the membrane-solution interface and hence higher solute separation in reverse osmosis.

Comparing the  $pK_1$  values of solutes 7, 9, and 13 with those of solutes 6, 2, and 14, no definite order is observed in their relative magnitudes. This means that the values of  $pK_1$  represent the polar character of carboxylate ion only with respect to solutes 7, 9, and 13. Hence, the values of  $\rho^*$  given earlier for aliphatic amino acids are not applicable for compounds containing additional polar substituents.

Table V gives the  $D_{AM}/K\delta$  data for films 5 and 6 at 250 psig with respect to the basic and acidic amino acids listed in Table I (solutes 26 to 30). The reverse osmosis experiments involving the basic amino acid solutes were conducted with equimolar quantities of HCl in their respective aqueous solutions to avoid pH values in the alkaline range. L-lysine exists in solution<sup>12</sup> predominantly as  $\text{NH}_3^+(\text{CH}_2)_4\text{CHNH}_2\text{COO}^-$ , so that it may be regarded as  $\epsilon$ -amino-*n*-caproic acid (solute 21) with an amino group substituted at the  $\alpha$ -carbon atom. L-aspartic acid exists in solution<sup>12</sup> predominantly as  $\text{COOHCH}_2\text{CHNH}_3^+\text{COO}^-$ , so that it may be regarded as DL-alanine (solute 2) with a —COOH group substituted at the  $\beta$ -carbon atom. Table V shows that the  $D_{AM}/K\delta$  values for all the three basic amino acids tested were less than the corresponding values for solute 21; similarly, the  $D_{AM}/K\delta$  values for the two acid amino acids tested were less than the corresponding values for solute 2. These results support the general conclusion that the effect of additional polar substitutions in the



TABLE V  
Separation of Some Basic and Acidic Amino Acids

Solute no.	Amino acid	$D_{AM}/K\delta$ of amino acid (cm/sec) $\times 10^5$		$D_{AM}/K\delta$ of amino acid hydrochloride, (cm/sec) $\times 10^5$		Solute separation, %	
		Film 5	Film 6	Film 5	Film 6	Film 5	Film 6
2	DL-Alanine	21.08	39.66			86.3 <sup>a</sup>	78.2 <sup>a</sup>
21	$\epsilon$ -Amino- <i>n</i> -caproic acid			45.85	79.78	71.3 <sup>b</sup>	59.6 <sup>b</sup>
26	L-Lysine			21.45	31.10	83.9 <sup>b</sup>	78.5 <sup>b</sup>
27	L-Arginine			20.95	28.82	83.6 <sup>b</sup>	78.9 <sup>b</sup>
28	L-Histidine			28.85	43.12	81.8 <sup>b</sup>	76.1 <sup>b</sup>
29	L-Aspartic acid	13.17	24.23			90.3 <sup>a</sup>	84.1 <sup>a</sup>
30	L-Glutamic acid	7.17	19.82			94.2 <sup>a</sup>	85.9 <sup>a</sup>

<sup>a</sup> Solute separation for amino acid.

<sup>b</sup> Solute separation for amino acid hydrochloride.

Operating pressure: 250 psig.

amino acid molecule is to reduce  $D_{AM}/K\delta$  values in reverse osmosis using cellulose acetate membranes.

### Separation of Aminobenzoic Acids in Aqueous Solutions

A few reverse osmosis experiments were carried out with aqueous solutions of *m*- and *p*-aminobenzoic acids (pH 4.15 and 4.05, respectively) and their hydrochlorides (pH 3.34 and 3.10, respectively) using films 5 and 6. An operating pressure of 250 psig was used for these experiments. The separations obtained for *m*-aminobenzoic acid were 18.3% and 11.1% with films 5 and 6, respectively, compared to practically no separation obtained for *p*-aminobenzoic acid. The separations obtained for *m*-aminobenzoic acid hydrochloride were 28.6% and 21.9% with films 5 and 6, respectively, compared to separations of 4.5% and 3.7% obtained respectively with films 5 and 6 for *p*-aminobenzoic acid hydrochloride. The higher separations for *m*-aminobenzoic acid and its hydrochloride are primarily due to the higher fraction of the dissociated species in the feed solution as shown by the dissociation data included in Table III for both the aminobenzoic acids studied.

Figure 10 illustrates the effect of pH of feed solution on degree of dissociation, and data on membrane performance with 0.001M *p*-aminobenzoic acid feed solutions at 500 psig using films 7 and 8. Table VI gives the data on the fraction of undissociated and dissociated species in the feed solutions used. Referring to Figure 10, there is a steep increase in solute separation in parallel with a steep increase in degree of dissociation in the pH range of 4.55 to 6.81. Solute separation passed through a minimum at the isoelectric pH at which solute separation was actually negative. Negligible or negative overall solute separations even when the degree of dissociation was 20% to 40% indicates that the undissociated species was preferentially sorbed at the membrane-solution interface during the experiment. Such solute preferential sorption may be expected to cause

TABLE VI  
Effect of pH on Dissociation of *p*-Aminobenzoic Acid

	pH 3.35 <sup>a</sup>	pH 3.57	pH 4.55	pH 5.15	pH 6.81
(R)/(R <sub>A</sub> )	0.777	0.791	0.608	0.323	0.011
(R <sup>+</sup> )/(R <sub>A</sub> )	0.083	0.051	0.004	~0	~0
(R <sup>-</sup> )/(R <sub>A</sub> )	0.024	0.041	0.298	0.629	0.987
(R <sup>±</sup> )/(R <sub>A</sub> )	0.115	0.117	0.090	0.048	0.002

<sup>a</sup> pH of feed solution.

Feed solution: 0.001 g-mole/l. of *p*-aminobenzoic acid.

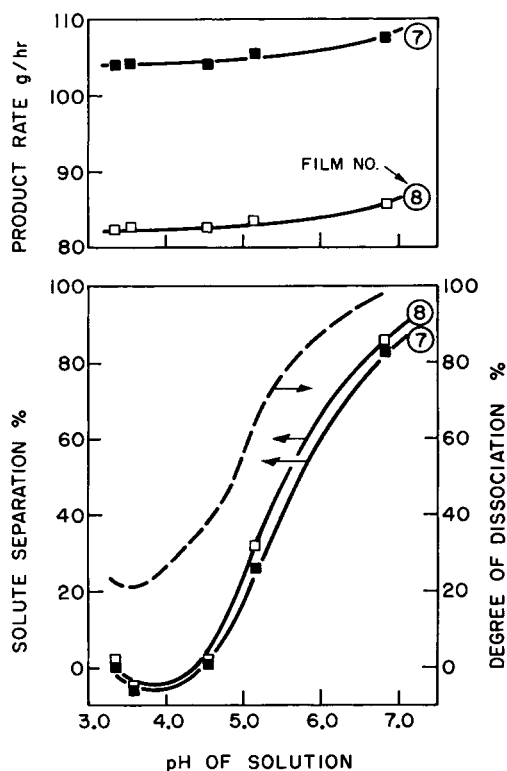


Fig. 10. Effect of pH on degree of dissociation, product rate, and solute separation for *p*-aminobenzoic acid. Film type, cellulose acetate, Batch 316 (10/30), operating pressure, 250 psig; feed concentration, 0.001 g-mole/l.; flow rate, 400 cc/min; membrane area, 7.6 cm<sup>2</sup>.

partial blocking of pores on the membrane surface, which would explain the increase in product rate with further increase in the degree of dissociation of the acid as seen in Figure 10.

### CONCLUSIONS

The reverse osmosis separation of amino acid ions in aqueous solution is governed by the combined effect of their polar ( $pK_1$ ) and steric ( $\Sigma E_s$ )

parameters. The solute transport parameter ( $D_{AM}/K\delta$ ) passes through a maximum (and hence solute separation passes through a minimum) at a  $pK_1$  value of 4.03 for completely ionized aliphatic amino acids containing no additional polar groups other than one  $-\text{COOH}$  and one  $-\text{NH}_2$  group. When the ions exist mostly as  $\text{R}^\pm$ , the steric parameter has a greater effect on solute separation; the effect of the polar parameter on solute separation increases with decrease in pH, and the consequent increase in the concentration of the ionic species  $\text{R}^+$ , in the feed solution. The data reported illustrate that the above effects can be predicted quantitatively. The effect of the presence of additional polar groups in the amino acid molecule is to increase its basicity and hence decrease its  $D_{AM}/K\delta$  value in reverse osmosis. The results of experiments with *m*- and *p*-aminobenzoic acids confirm that solute separation increases with increase in the overall degree of dissociation and further indicate that the undissociated *p*-aminobenzoic acid is preferentially sorbed at the membrane-solution interface. The reverse osmosis data with all the amino acids studied indicate that with respect to each ionic species, solute separation is in the order  $\text{R}^- > \text{R}^\pm > \text{R}^+$  for the cellulose acetate membrane material used.

### Nomenclature

$A$	pure water permeability constant, g-mole $\text{H}_2\text{O}/\text{cm}^2$ sec atm
$C^*$	proportionality factor depending on the porous structure of the membrane surface, cm/sec
$d$	solution density, $\text{g}/\text{cm}^3$
$D_{AB}$	diffusivity of amino acid, $\text{cm}^2/\text{sec}$
$(D_{AB})_{\text{ref}}$	diffusivity of sodium chloride, $\text{cm}^2/\text{sec}$
$D_{AM}/K\delta$	solute transport parameter, cm/sec
$f$	fraction solute separation
$(\text{H}^+)$	proton concentration, g-mole/l.
$k$	mass transfer coefficient on the high-pressure side of the membrane, cm/sec
$k_{\text{ref}}$	mass transfer coefficient on the high-pressure side of the membrane for the reference solution system 1500 ppm $\text{NaCl}-\text{H}_2\text{O}$ , cm/sec
$K_1$	equilibrium constant defined by eq. (5), g-mole/l.
$K_2$	equilibrium constant defined by eq. (6), g-mole/l.
$K_a$	dissociation constant of amine, g-mole/l.
$K_A$	equilibrium constant between $\text{R}^+$ and $\text{R}^\pm$
$K_B$	equilibrium constant between $\text{R}^+$ and $\text{R}$
$K_C$	equilibrium constant between $\text{R}^\pm$ and $\text{R}^-$
$K_D$	equilibrium constant between $\text{R}$ and $\text{R}^-$
$K_E$	equilibrium constant defined by eq. (7)
$M$	molecular weight of solvent (=18.02 for water)
$pK_1$	$-\log K_1$ used as polar parameter
$PR$	product rate, grams per hour per given area of film surface
$PWP$	pure water permeability, grams per hour per given area of film surface

(R)	concentration of the undissociated species, g-mole/l.
(R <sup>+</sup> )	concentration of the positively charged species, g-mole/l.
(R <sup>-</sup> )	concentration of the negatively charged species, g-mole/l.
(R <sup>±</sup> )	concentration of the zwitter ion, g-mole/l.
(R <sub>A</sub> )	total concentration of the amino acid, g-mole/l.
$R_{pK_1}^2$	fraction of total variance of $\ln(D_{AM}/K\delta)$ related to $pK_1$
$R_{\Sigma E_s}^2$	fraction of total variance of $\ln(D_{AM}/K\delta)$ related to $\Sigma E_s$
$S$	effective membrane area, cm <sup>2</sup>
$T$	temperature, °K
$V_1$	molal volume of solute at normal boiling point, cm <sup>3</sup> /g-mole

#### Greek Letters

$\delta^*$	steric coefficient
$\mu$	viscosity of solution, centipoise (=0.8937 for pure water)
$\rho^*$	polar coefficient
$\sigma^*$	Taft's polar parameter
$\Sigma E_s$	Taft's steric parameter
$\chi$	"association" parameter of solvent (=2.6 for water)

Issued as N. R. C. No. 14215

#### References

1. T. Matsuura and S. Sourirajan, *J. Appl. Polym. Sci.*, **15**, 2905 (1971).
2. T. Matsuura and S. Sourirajan, *J. Appl. Polym. Sci.*, **16**, 1663 (1972).
3. T. Matsuura and S. Sourirajan, *J. Appl. Polym. Sci.*, **17**, 3661 (1973).
4. C. Kamizawa, H. Masuda, and S. Ishizaka, *Bull. Chem. Soc. Japan*, **45**, 2964 (1972).
5. B. Kunst and S. Sourirajan, *J. Appl. Polym. Sci.*, **14**, 2559 (1970).
6. L. Pageau and S. Sourirajan, *J. Appl. Polym. Sci.*, **16**, 3185 (1972).
7. S. Sourirajan, *Reverse Osmosis*, Academic Press, New York, 1970, Chap. 3.
8. T. Matsuura and S. Sourirajan, *J. Appl. Polym. Sci.*, **17**, 1043 (1973).
9. C. R. Wilke and P. Chang, *A.I.Ch.E.J.*, **1**, 264 (1955).
10. R. H. Perry, C. H. Chilton, and S. D. Kirkpatrick, Eds., *Perry's Chemical Engineers' Handbook*, 4th ed., McGraw Hill, New York, 1963, pp. 14-20.
11. *Handbook of Chemistry and Physics*, C. D. Hodgman, Ed., 43rd ed., The Chemical Rubber Pub. Co., Cleveland, Ohio, 1961, p. 2229.
12. J. P. Greenstein and M. Winitz, *Chemistry of the Amino Acids*, Vol. 1, John Wiley & Sons, New York, 1961, Chap. 4.
13. T. Kaneko, T. Shiba, and T. Inui, in *Handbook of Organic Structural Analysis*, Y. Yukawa, Ed., W. A. Benjamin, New York, 1965, pp. 631-634.
14. T. Matsuura, M. E. Bednas, J. M. Dickson, and S. Sourirajan, *J. Appl. Polym. Sci.*, **18**, 2829 (1974).
15. R. W. Taft, Jr., in *Steric Effects in Organic Chemistry*, M. S. Newman, Ed., Wiley, New York, 1956, p. 598.
16. W. V. Valkenburg, *Advan. Chem. Ser.* **114**, 36 (1972).
17. W. L. Gore, *Statistical Methods for Chemical Experimentation*, Interscience, New York, 1952, Chap. VI.
18. W. M. King, D. L. Hoernschemeyer, and C. W. Saltonstall, Jr., in *Reverse Osmosis Membrane Research*, H. K. Lonsdale and H. E. Podall, Eds., Plenum, New York, 1972, p. 131.
19. T. Matsuura, M. E. Bednas, and S. Sourirajan, *J. Appl. Polym. Sci.*, **18**, 567 (1974).

Received February 28, 1974

Revised May 8, 1974